

Small Scale Structure in the Universe and the Distribution of Baryons at High Redshift

Michael Rauch

*Astronomy Department 105-24
California Institute of Technology
Pasadena, CA 91125, USA
e-mail: mr@astro.caltech.edu*

Abstract.

We discuss briefly the relevance of Lyman α forest observations for measuring cosmological parameters, comparing the properties of high z Keck QSO spectra with those of artificial spectra from hydrodynamic simulations, based on hierarchical cosmologies. In particular, we describe a measurement of the baryon content of the universe obtained by matching the average opacity of the Lyman α forest from simulations to the observed one from a new dataset observed with the Keck telescope. For conservative assumptions about the intensity of the UV background we obtain a lower limit $\Omega_b h^2 > 0.017$. Searching for column density gradients in absorption systems common to adjacent gravitationally lensed quasar images we test for the presence of sub-kpc clumpiness which could invalidate the results of simulations with limited resolution. We find that in those Ly α forest clouds dominating the mean absorption, such structure, if present, cannot exceed the 4 percent level (over 100 – 200 pc). Extending the study of lensed absorption to higher column densities we begin to sample the velocity field internal to high redshift galaxies. Remarkable differences in column density (of order 50 %) and projected velocity (tens of km/s) between lines of sight separated by only a few hundred parsecs are found, and we may be observing structure in the early interstellar medium.

It is obvious from the wide range of contributions to this meeting that observations and especially the theory of the intergalactic medium have made substantial progress during the past few years. Bright QSO spectra with signal-noise ratios of order 100 and a resolution of 5 km/s (FWHM) can now be obtained routinely in a few hours with the Keck and soon with other large telescopes. Cosmological hydro-simulations have advanced our understanding of the Ly α forest phenomenon to a point where quantitative cosmology with the IGM has come within reach (see also the contributions by Bond, Croft, Davé, Davidsen, Gnedin, Hui, Meiksin, Miralda-Escudé, Muecket, Weinberg, at this conference) and even the study of galaxy formation in absorption is now becoming possible (talks by Haehnelt, Hellsten, Murakami, Steinmetz).

1 The Lyman α Forest - Observing the Main Baryonic Reservoir

Observations of the Ly α forest provide a very sensitive way for observing of the cosmic matter distribution and the early stages of galaxy formation: this is because the *linear density regime* of gravitational collapse near turnaround for galactic scales (several hundred kpc at $z \sim 3$) coincides roughly with the *linear*

part of the curve of growth for the Lyman α absorption line, as shown in fig. 1. The hydro-simulations picture a Ly α forest caused by a coherent network

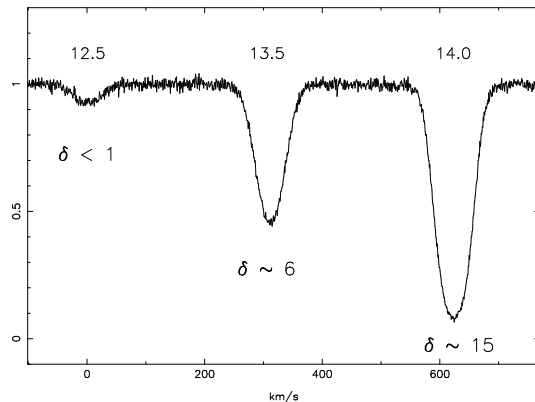


Figure 1: The observable range of the linear part of the curve of growth. The logarithmic column densities and corresponding typical baryonic overdensities δ are shown for three artificial $z=3$ HI Ly α lines.

of filaments, sheets, and knots of gas, in which more spherical, higher density condensations, galaxies or mini-halos, are embedded. The fraction of baryons in Lyman α clouds in CDM based models is indeed very high [7], with (even by $z \sim 2$) of order 80% of all baryons in low column density clouds, dominated by the range ($14 < \log N < 15.5$) [6],[4]. The spatial arrangement of this baryonic reservoir is illustrated by fig. 2. Column density contours at a level as high as 10^{14} cm^{-2} are stretching continuously over many hundreds of kpcs. *Most of the baryons are concentrated in the filaments*, without having collapsed into Lyman limit systems, virialized galaxies or damped Ly α systems yet.

2 The Baryon Content of the Universe

The hydrodynamic simulations are illustrative and have furthered the interpretation of QSO absorption spectra immensely, but they can also be used for quantitative measurements, e.g., by comparing large sets of simulated QSO spectra with observed ones. The problem is as usual to find observables which can be measured at a reasonable precision, do not depend sensitively on the shortcomings of the modelling and at the same time correspond in a unique way to the ingredients of the simulated model.

One of the most easily measurable quantities is the distribution of pixel intensities $I = e^{-\tau}$ (or alternatively, flux decrements $D = 1 - I$, or optical depths τ), i.e. the amount of light per unit velocity absorbed by Ly α of intervening HI clouds from the beam of a QSO. The optical depth τ is a measure of the distribution of the neutral hydrogen in real and velocity space,

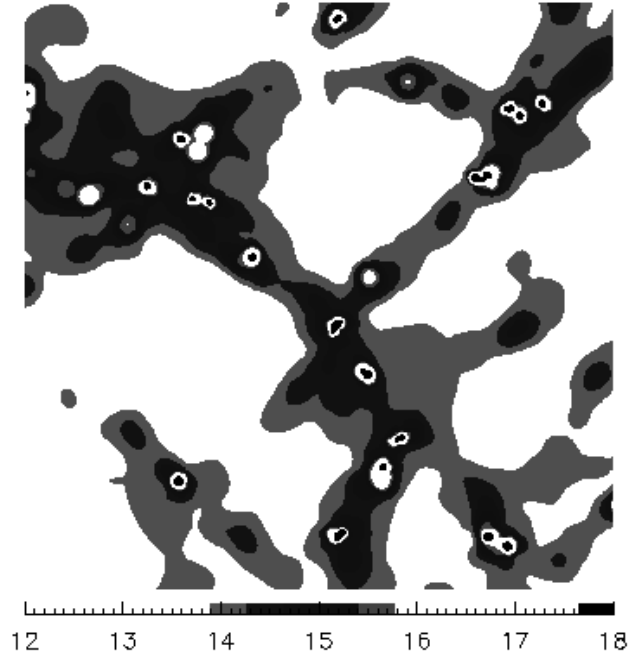


Figure 2: The projected HI column density distribution in a cube of size 700 kpc (proper), at $z=3.1$, from a standard CDM SPH simulation by M. Steinmetz. The contours refer to $\log N(\text{HI})$.

$\tau \propto dN_{\text{HI}}/dv$, where dN_{HI} is the neutral hydrogen column density spread out over velocity interval dv . The simulations predict density ρ , temperature T , peculiar velocity v_{pec} , and thus the ionization state of the gas as a function of the cosmological model, with the ionizing radiation background, and the total Ω_b in the universe as free parameters. In the density range producing most of the absorption the gas is highly ionized, and photoionization dominates the ionization equilibrium. Then the optical depth for absorption is approximately proportional to

$$\tau \propto \frac{(\Omega_b H_0^2)^2}{\Gamma H(z)} (1+z)^6 \alpha(T) \left(\frac{\rho}{\bar{\rho}}\right)^2 \left(1 + \frac{dv_{\text{pec}}}{H(z)dr}\right)^{-1}, \quad (1)$$

where Γ is the photoionization probability per second, $\alpha(T)$ the recombination coefficient, $H(z)$ the Hubble constant, ρ the gas density, and dv_{pec}/dr the gradient of the peculiar velocity along the line of sight.

Then, for a given temperature, the optical depth scales with $\Omega_b^2 h^4 / (H(z)\Gamma)$. If we are able to obtain an independent estimate of one of the parameters e.g., the ionizing flux, we can determine the other, e.g., $\Omega_b h^{3/2}$ or vice versa.

We have observed a sample of 7 QSOs with the Keck telescope, and compared the observed distribution of flux decrements $D = 1 - e^{-\tau}$ with the predicted distribution from an Eulerian hydro-simulation of a CDM+ Λ universe [1], and a standard CDM universe from an SPH simulation [4]. The measurement consists of applying a suitable global scaling to the simulated optical depths such that the mean flux decrements agree between simulation and observation for each of three redshift bins,

$$\overline{D}_{obs}(z) = \overline{D}_{sim}(z), \quad z = 2, 3, 4. \quad (2)$$

Observed and simulated cumulative flux decrement distributions are shown in fig. 3. The continuum level is at $D = 0$, the zero level (no transmitted light) at $D = 1$. One remarkable feature is the rapid decrease of the mean absorption with decreasing redshift. In the hierarchical models this is mostly due to the expansion of the universe which decreases the gas density and the neutral fraction. Excellent agreement with the observed distribution is attained for both models, after scaling the optical depth globally. It is worth pondering that this is the result of a one-parameter fit which is equivalent to adjusting the area under the curve giving the cumulative distribution. The agreement between the shapes of the distribution is an independent bit of information, telling us that these models do indeed produce a Ly α forest with a realistic intensity distribution. The Eulerian Λ CDM model is doing slightly better than the SPH SCDM simulation, in that the latter has more absorption at low column densities, leading to a steeper slope than observed. This may reflect differences in the way the heating during reionization was incorporated.

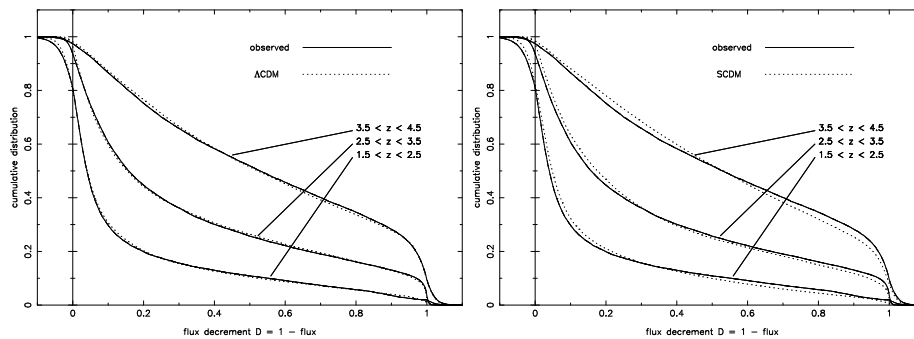


Figure 3: left: Comparison between observed (solid line) and simulated (best fit: dotted line) cumulative flux decrement distribution for the CDM+ Λ model of [1]. right: Same statistic for the standard CDM SPH simulation of [4])

Having obtained the scalefactors for the optical depths in the simulations we can derive a lower limit on Ω_b . For an independent estimate of the radiation

background intensity we adopt a temporally constant UV background with $\Gamma > 7 \times 10^{-13} \text{ s}^{-1}$. This value corresponds to $J_\nu \approx 2.3 \times 10^{-22}$ (depending on the spectral shape). It is a *lower limit* in that it includes only the radiation background from known QSOs alone. From the firm lower limit on Γ due to QSOs alone we can determine a lower limit for the amount of baryons in the universe:

$$\Omega_{baryon} h^2 > 0.017$$

Our measurement (described in more detail in [8]) supports a high Ω_{baryon} (low D/H) universe, still consistent with the upper range permitted by the solar system light element abundances [3] and with the Ω_{baryon} derived from the D/H measurements by Tytler et al. (these proceedings). Remaining uncertainties stem from the assumed intensity of the ionizing radiation background, and the temperature the lower column density gas has attained by the time reionization is complete. Moreover, the data sample is still relatively small, especially at lower redshifts.

The validity of these results depends of course not only the correct cosmological model, but also on its technical realisation: how can we be sure that we are not missing structure on very small scales, which are not resolved by the simulations? If there were clumpiness on sub-kpc scales (unresolved by current techniques), the gas could be locally more neutral and a smaller amount of baryons could conceivably account for the same amount of opacity in the Lyman α forest. From some point on such structure will diverge from the properties of the CDM based cosmological models [12] but the only way to find out for sure whether it exists is to search directly for clumpiness in the gas responsible for most of the Ly α forest absorption.

3 Density Gradients on Sub-Kpc Scales

The presence or absence of density and velocity structure on very small scales at high z can best be tested for by searching for differences between the absorption systems in adjacent lines of sight to multiple (lensed) QSO images. We have embarked on a project to (re-)observe high redshift lensed QSOs with the Keck HIRES spectrograph, among them the two cases UM 673 and HE 1104-1805, studied in the important papers by Smette et al. ([9, 10]). The difference to earlier work is that with Keck we are able to resolve the line widths even of most metal absorption systems, and can measure the column densities directly.

The column density differences over a known separation in the plane of the sky can be translated into gradients in the baryon density. We have completely profile-fitted a Lyman α forest region around $z= 2.6$ in both the *A* and *B* images of the QSO UM673 and measured the column differences among those Voigt profile components agreeing in velocity position to within 10 km s^{-1} . We restricted the analysis to HI column densities between 10^{12} and 10^{14} cm^{-2} , a range contributing most prominently to the opacity at redshifts 2.6. This way

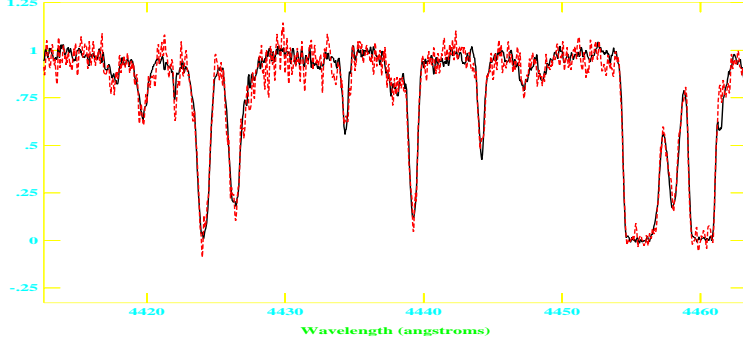


Figure 4: Ly α forest near $z=2.64$ in the line of sight to UM673 (transverse separation $0.11 h_{50}^{-1}$ kpc). The solid line is the spectrum of the A image, the dotted one that of the B image. The only discernible difference between the spectra comes from an MgI line at $z=0.563$ on the RHS of the rightmost Ly α complex only visible in the A image (separation $13.9 h_{50}^{-1}$ kpc)

we should be able to answer our question whether there is structure in the gas producing the Ly α forest which may be capable of upsetting the Ω_b results. It has been argued [2, 5] that the HI column density $N(\text{HI})$ should depend on the baryon density as

$$N(\text{HI}) \propto \rho^\alpha$$

with $\alpha \approx 1.6$. For the RMS scatter of the logarithmic baryon density gradient we then obtain

$$\left\langle \left(\frac{d \log \rho}{dr} \right)^2 \right\rangle \leq \alpha^{-2} \left\langle \left(\frac{|\log N_A - \log N_B|}{dr} \right)^2 \right\rangle \quad (3)$$

The inequality arises because the variable thickness of the clouds introduces an additional scatter in the column densities, even for a density field constant everywhere. Retaining only those line pairs with a measurement error of less than 0.2 in the logarithmic column density differences we arrive at an upper limit to the RMS estimate for fluctuations in the logarithmic overdensity,

$$\sqrt{\left\langle (\Delta \log \rho)^2 \right\rangle} \leq 3.6 \times 10^{-2}, \quad 12.0 \leq N(\text{HI}) \leq 14.0 \text{ cm}^{-2} \quad (4)$$

valid for a sample with a mean transverse separation of $0.16 h_{50}^{-1}$ kpc between the lines of sight (for $q_0=0.5$). Other choices of sample size give similar values. Obviously, those parts of the universe contributing most to the Ly α forest opacity do not show detectable clumpiness, at least on the scale we have now searched. Future investigations of lenses with somewhat wider image separation and/or wavelength coverage further to the blue will eventually provide information on the kpc range.

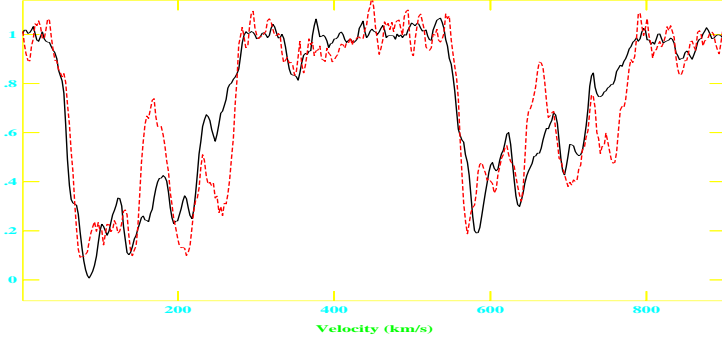


Figure 5: CIV ($\lambda\lambda$ 1548, 1551 \AA) complex at $z=2.35$ towards UM673 (LOS separation $0.68 h_{50}^{-1}$ kpc).

4 Velocity and Density Fields in Protogalaxies

Moving to higher column densities the lines of sight ultimately must be sampling the gaseous extent of high redshift galaxies. The presence of these can be inferred from the striking variations between metal absorption lines in the different images, which stand out quite dramatically from the quiescent lower column density $\text{Ly}\alpha$ forest. Column densities even in the high ionization CIV gas can fluctuate by a factor two over a few hundred parsecs (Fig. 5). Apparently, we are seeing variations in the ionization parameter of the early interstellar medium. These variations can be used to establish the sizes (more correctly the coherence lengths) for the gas units in those galaxies, and the internal velocity dispersion.

Fig. 6 shows for the first time, how the decoherence in the properties of these CIV absorption systems takes place in individual lines of sight as a function of beam separation. In this figure each CIV complex (i.e., the full absorption system) is shown by a large circle. "Subclumps", i.e., groups of lines, between which the continuum recovers, have been assigned by eye somewhat subjectively, and are denoted by small circles. Individual absorption components, as far as their fate can be traced across the lines of sight, are represented by dots. The different classes of symbols are of course not statistically independent as the single components are parts of the subclumps etc. It is obvious from the LHS figure that variations in the column density of individual CIV components have reached 50% at separations of a few hundred pc, while the total complexes differ at that level once separations between a few and 20 kpc are reached. Velocity differences increase to about 60 km^{-1} at separations of a few kpc (RHS plot). As one goes to the very smallest separations the differences both in velocity and column density do not diminish as much as expected for a naive extrapolation to zero separation at the QSO redshift

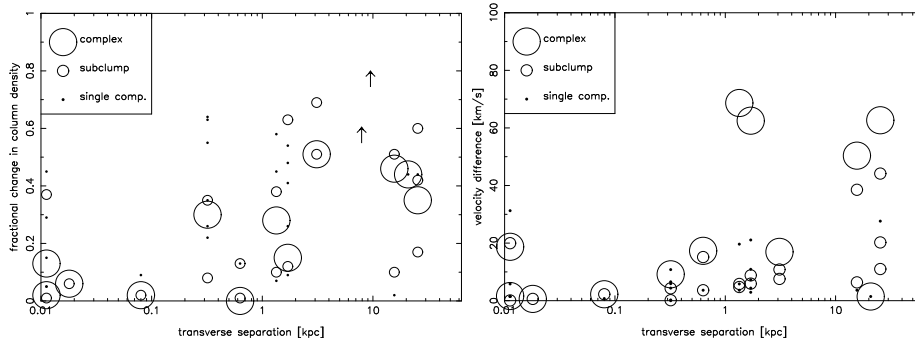


Figure 6: Fractional difference in column density (left), and the difference in the column density weighted velocity (right) between the two lines of sight as a function of transverse separation. Large circles represent whole CIV complexes (arrows are lower limits), small circles "subclumps", and the dots stand for single components.

itself. This may be indicating that the associated ($z_{abs} \approx z_{em}$) clouds are smaller than intervening systems, do not cover the QSO continuum emission region, or possess some internal motion on very small scales.

We can use the differences in column density as a function of separation to estimate, in a statistical sense, the size of the CIV absorbing galaxies as a function of the column density detection threshold. Making the very crude assumption that all these objects have identical sizes and densities, and approximating their column density – radius relation by a Gaussian, we find a mean radius of $14 h_{50}^{-1}$ kpc at the $3.7 \times 10^{12} \text{cm}^{-2}$ ($\sim 15 \text{m}\text{\AA}$ equivalent width) contour. We emphasize that this is a very crude estimate as it appears already from the few systems observed that there is a whole range of sizes. Interestingly, this coherence length for high ionization gas (at $z \approx 2-3$) is considerable smaller than that for MgII (low ionization) systems at low redshifts and similar detection threshold ($\sim 180 h_{50}^{-1}$ kpc for $0.5 < z < 1.3$; [13]). The increase in cross-section could be due to galaxy halos growing, or an increasing metal enrichment of the universe by volume, as time proceeds.

Acknowledgements. The Ω_b measurement is the result of an ongoing collaboration with J. Miralda-Escudé, W.L.W. Sargent, T. A. Barlow, D.H., Weinberg, L. Hernquist, N. Katz, R. Cen, and J.P. Ostriker, to be published in greater detail in the ApJ Nov. 1997 issue. The work on lenses is done in collaboration with W.L.W. Sargent and T. A. Barlow. The observations were made at the W.M. Keck Observatory which is operated as a scientific partnership between the California Institute of Technology and the University of California; it was made possible by the generous support of the W.M. Keck Foundation. I am grateful to M. Steinmetz for providing the column density plot from his simulation (fig. 2), and to NASA for support through grant HF-01075.01-94A from the Space Telescope Science Institute.

References

- [1] Cen, R., Miralda-Escudé, J., Ostriker, J.P., Rauch, M., 1994, *ApJ*, 437, L9
- [2] Croft, R.A.C., Weinberg, D.H., Katz, N., Hernquist, L., 1997, *ApJ*, in press (astro-ph 96011053)
- [3] Hata, N., Steigman, G., Bludman, S., Langacker, P., 1997, *Phys. Rev. D*, 55, 540
- [4] Hernquist L., Katz N., Weinberg D.H., Miralda-Escudé J., 1996, *ApJ*, 457, L5
- [5] Hui, L., & Gnedin, N. Y. 1997, *MNRAS*, in press, (astro-ph/9612232)
- [6] Miralda-Escudé J., Cen R., Ostriker J.P., Rauch M., 1996, *ApJ*, 471, 582
- [7] Petitjean, P., Webb, J.K., Rauch, M., Carswell, R.F., Lanzetta, K., 1993, *ApJ*, 262, 499
- [8] Rauch, M., Miralda-Escudé, J., Sargent, W. L. W., Barlow, T. A., Weinberg, D. H., Hernquist, L., Katz, N., Cen, R., Ostriker, J. P., 1997, *ApJ*, in press (astro-ph/9612245)
- [9] Smette, A., Surdej, J., Shaver, P. A., Foltz, C. B., Chaffee, F. H., Weymann, R. J., Williams, R. E., & Magain, P. 1992, *ApJ*, 389, 39
- [10] Smette, A., Robertson, J. G., Shaver, P. A., Reimers, D., Wisotzki, L., & Köhler, Th. 1995, *A&AS*, 113, 199
- [11] Tytler D., Fan, X.M, Burles, S. 1996, *Nature*, 381, 207
- [12] Weinberg D.H., Miralda-Escudé J., Hernquist L., Katz N., 1997, *ApJ*, in press, (astro-ph 9701012)
- [13] Womble D.S., in Meylan G. (ed.): *QSO Absorption Lines*, 1995, Springer, Berlin, p. 157